

Pion-Nucleon Coupling at Finite Temperature

C. A. Dominguez^(a), C. van Gend^(a), and M. Loewe^(b)

^(a)Institute of Theoretical Physics and Astrophysics
University of Cape Town, Rondebosch 7700, South Africa

^(b)Facultad de Fisica, Pontificia Universidad Catolica de Chile
Casilla 306, Santiago 22, Chile

Abstract

The pion nucleon vertex function at finite temperature is studied in the framework of: (a) the thermal (linear) sigma model to leading (one-loop) order, and (b) a thermal QCD-Finite Energy Sum Rule. Results from both methods indicate that the strength of the pion-nucleon coupling decreases with increasing T , vanishing at a critical temperature. The associated mean-square radius is a monotonically increasing function of T , diverging at the critical temperature. This is interpreted as (analytical) evidence for the quark-gluon deconfinement phase transition.

The temperature behaviour of hadronic Green's functions, and their associated parameters such as masses, widths, couplings, etc., has received considerable attention lately, given its impact on the search for the quark-gluon plasma [1]. Two successful theoretical frameworks for these studies are the thermal sigma model [2]-[4], and QCD sum rules [5]-[6]. The former technique provides information on the T -dependence of pion and nucleon masses and widths associated, respectively, with the real and imaginary parts of their two-point Green's functions. While these masses show no appreciable variation with temperature, [2]-[3] their widths exhibit a dramatic increase with increasing T [2],[4]. This result is in line with the expectation that hadronic widths, interpreted as absorption coefficients in the thermal bath, should diverge at some critical temperature [7]. This provides a signal or phenomenological order parameter for the quark-gluon deconfinement phase transition. Another such signal is the thermal behaviour of hadronic couplings and form factors (three-point functions), which should vanish at a critical temperature, where the associated mean square radii should diverge. This has been explicitly confirmed for the electromagnetic form factor of the pion [8], and for the rho-pi-pi coupling [9]. In this note we study the πNN vertex function at finite temperature using the thermal (linear) sigma model, as well as QCD sum rules. The purpose is to obtain additional confirming (analytical) evidence for the deconfinement phase transition, as well as information on this vertex function, which should be of use in hadron gas models at finite temperature.

We begin with the (linear) sigma model, and consider the πNN vertex

$$\Gamma(q^2) = V(q^2)\bar{u}_f(p')\gamma_5\tau_\alpha u_i(p) \quad (1)$$

where the nucleons are on-mass shell, and the pion has virtual mass $q^2 = (p' - p)^2$. The renormalization of the sigma model (at $T = 0$) is discussed e.g. in [10], and the renormalization of the πNN vertex (before the invention of dimensional regularization and the $\bar{M}\bar{S}$ scheme) may be found in [11]. At finite temperature we shall use the Dolan-Jackiw real time propagators [12], together with the fact that thermal corrections do not induce any new kind of ultraviolet corrections. Hence, the thermal theory may be renormalized as at $T = 0$. We have done this using dimensional regularization and the $\bar{M}\bar{S}$ scheme. To leading (one-loop) order, the relevant diagrams are shown in Fig. 1 (a-e). At the kinematical point $q^2=0$, and in the chiral limit, the expression for the irreducible vertex $V(q^2)$ is given

by

$$V(0) = g(1 + \beta(0)g^2) \quad (2)$$

where

$$\begin{aligned} \beta(0) = & \frac{1}{16\pi^2} \left[-\frac{5}{3} \frac{M_\sigma^2}{M_N^2} + \frac{M_\sigma^2}{M_N^2} \left(3 - \frac{5}{6} \frac{M_\sigma^2}{M_N^2} \right) \ln \frac{M_\sigma^2}{M_N^2} \right. \\ & \left. + \frac{1}{3} (5M_\sigma^2 - 8M_N^2) \frac{M_\sigma}{M_N^4} \sqrt{4M_N^2 - M_\sigma^2} \arctan \frac{\sqrt{4M_N^2 - M_\sigma^2}}{M_\sigma} \right] \end{aligned} \quad (3)$$

with M_N and M_σ being the nucleon and sigma meson masses, respectively. Equation (2) may be regarded as an expression for the effective coupling constant $g_{\pi NN}$ in the chiral limit. It is equal to g if $\beta(0)$ vanishes. This happens for $M_\sigma \simeq 1300 \text{ MeV}$; in fact, $\beta(0)$ is small and negative if M_σ is bigger than this value. One should recall that in the linear sigma model $g_A = 1$, so that the Goldberger-Treiman relation (GTR) [13] becomes: $M_N = g f_\pi$. Using the chiral symmetry limit values [14]: $M_N \simeq 800 \text{ MeV}$, and $f_\pi \simeq 80 \text{ MeV}$, one finds: $g \simeq 10$, not far from the experimental value $g_{\pi NN} \simeq 13$. In any case, here we are only interested in the temperature behaviour of the *ratio* $V(q^2, T)/V(q^2, 0)$; particularly in the possibility that this ratio vanishes at a critical temperature, and that the mean square radius diverges there. This will turn out to be largely independent of the particular value assumed by g or $g_{\pi NN}$ and $\beta(0)$ (or equivalently M_σ), although the specific value of the critical temperature does depend on the latter.

Turning to the temperature corrections to the graphs shown in Fig. 1, we need only consider Fig. 1(b) and Fig. 1(d) (identical to Fig. 1(e)), as Fig. 1(c) is Boltzmann suppressed on account of $M_N \simeq M_\sigma \gg \mu_\pi$. The thermal correction to the graph Fig. 1(b) is given by

$$\Gamma(q^2, T) = -g^3 \bar{u}_f(p') \gamma_5 \tau_\alpha u_i(p) \int \frac{d^4 k}{(2\pi)^4} \frac{k^2 n_B(k_0) \delta(k^2 - \mu_\pi^2)}{[(p' - k)^2 - M_N^2][(p - k)^2 - M_N^2]} \quad (4)$$

where n_B is the Bose thermal factor: $n_B(z) = (e^{z/T} - 1)^{-1}$. Hence, this contribution vanishes in the chiral limit. That of Fig. 1(d) is found to be

$$\Gamma(q^2, T) = g^3 \frac{(M_\sigma^2 - \mu_\pi^2)^2}{2f_\pi^2 M_N} \bar{u}_f(p') \gamma_5 \tau_\alpha \int \frac{d^4 k}{(2\pi)^4} \frac{(2m_N - \not{k}) 2\pi \delta(k^2) n_B(k_0)}{[(k+q)^2 - M_\sigma^2][(p-k)^2 - M_N^2]} u_i(p) \quad (5)$$

We choose for convenience a Lorentz frame in which the incoming nucleon is at rest with respect to the heat bath ($\vec{p} = 0$). We have checked that the final results are largely independent of the choice of frame. The thermal effective πNN coupling in the chiral limit, and at $q^2=0$, may then be written as

$$\frac{V(0, T)}{V(0, 0)} = 1 - \frac{g^2 T^2}{12M_N^2(1 + g^2 \beta(0))} \quad (6)$$

where the GTR has been used. Notice that an extrapolation in temperature of this result implies a critical temperature

$$T_d = \sqrt{12(1 + \beta(0)g^2)} M_N / g \quad (7)$$

which depends on the value of the sigma-meson mass through $\beta(0)$; numerically, $T_d \simeq 150 - 300 \text{ MeV}$ if $M_\sigma \simeq 1300 - 1600 \text{ MeV}$. One should not assign too much importance to the specific numerical values of this critical temperature and/or the sigma-meson mass, to wit. First, the relations among parameters in the sigma model are valid at the 25-30% level; e.g. $g_A = 1$ instead of the experimental value $g_A = 1.26$, and $g_{\pi NN} \simeq 10$ (from the GTR), as opposed to the experimental value $g_{\pi NN} \simeq 13$, etc.. Second, Eq.(6) and the T^2 dependence is a consequence of the one-loop approximation. Higher loop corrections will induce higher order (in T) terms which will alter the numerical value of the critical temperature. These will be suppressed, though, by inverse powers of the nucleon/sigma-meson masses. A similar situation arises in chiral perturbation theory and the T -dependence of the pion decay constant $f_\pi(T)$. To order T^2 , $f_\pi(T)$ vanishes at $T_c \simeq 240 \text{ MeV}$ [15], while higher order corrections bring down this value considerably. What we find important here, is that the πNN coupling at leading order in T decreases with increasing temperature.

Next, we consider the mean-square radius associated with $V(q^2, T)$, and defined as

$$\frac{\langle r_{\pi NN}^2 \rangle_T}{\langle r_{\pi NN}^2 \rangle_0} = \frac{V(0,0)}{V(0,T)} \left[\frac{\partial V(q^2, T)}{\partial q^2} \bigg/ \frac{\partial V(q^2, 0)}{\partial q^2} \right] \bigg|_{q^2=0} \quad (8)$$

We have calculated this ratio numerically, the result being shown in Figure 2. An extrapolation in temperature indicates quite clearly the divergence of this mean square radius. This may be interpreted as a signal for deconfinement, to the extent that the *size* of the nucleon, as probed by a pion, increases with increasing temperature, becoming infinite at $T = T_d$.

We study next the same vertex function, but in the framework of QCD Finite Energy Sum Rules (FESR). This will provide important independent support to the above result, especially since the QCD sum rule technique, unlike the sigma model, does not entail any expansion in powers of the temperature. To this end, we begin the analysis at zero temperature and introduce the three-point function

$$\Pi(p, p', q) = i^2 \int d^4x \, d^4y \langle 0 | T(\eta(x) J_5(y) \bar{\eta}(0)) | 0 \rangle e^{i(p' \cdot x - q \cdot y)} \quad (9)$$

where the nucleon and pion interpolating currents, $\eta(x)$ and $J_5(x)$, respectively, are chosen as

$$\eta(x) = \epsilon_{abc} \left[u^a(x) C \gamma_\mu u^b(x) \right] \gamma^\mu \gamma_5 d^c(x) \quad (10)$$

$$J_5(x) = i \left[\bar{u}(x) \gamma_5 u(x) - \bar{d}(x) \gamma_5 d(x) \right] \quad (11)$$

where C is the charge conjugation operator. The couplings of these currents to the nucleon and the pion are defined as

$$\langle 0 | \eta(0) | N(p, s) \rangle = \lambda_N u(p, s) \quad (12)$$

$$\langle N(p_2, s_2) | J_5(0) | N(p_1, s_1) \rangle = \bar{u}(p_2, s_2) \gamma_5 g_P(q^2) u(p_1, s_1) \quad (13)$$

where

$$g_P(q^2) = \frac{f_\pi \mu_\pi^2}{m_q} \frac{g_{\pi NN}}{q^2 - \mu_\pi^2} \quad (14)$$

and where m_q is the average of the up and down quark masses. In our normalization, the pion decay constant is $f_\pi \simeq 93 \text{ MeV}$. The hadronic representation of the imaginary part of the vertex function Eq. (9) is obtained by inserting a complete set of hadronic states. After summing over spins, and making the standard nucleon-pole approximation (thus including in the continuum all the radial excitations of the nucleon) one obtains

$$\begin{aligned} \text{Im}\Pi(s, s', q^2)|_{\text{HAD}} &= g_P \lambda_N^2 M_N (i\gamma_5 \not{q}) \pi^2 \delta(s - M_N^2) \delta(s' - M_N^2) \\ &\quad + \theta(s - s_0) \theta(s' - s'_0) \text{Im}\Pi(s, s', q^2)|_{\text{QCD}} \end{aligned} \quad (15)$$

Since we are interested in the pion-nucleon coupling in the vicinity of $q^2=0$, we can safely neglect any q^2 dependence in $g_{\pi NN}$. This dependence would arise from the contribution of the radial excitations of the pion, $\pi'(1300)$ etc., which in the chiral limit is a correction of order q^2/M_π^2 . As usual, the hadronic continuum with thresholds s_0 and s'_0 is modelled by the QCD spectral function. The leading order diagrams needed to compute the latter are shown in Fig. 3. In the chiral limit, the relevant structure to be sought is proportional to $q\bar{q}$. It turns out that the diagram Fig. 3a does not have this behaviour, while that of Fig. 3b (plus all other related diagrams) gives

$$\text{Im}\Pi(s, s', q^2)|_{\text{QCD}} = \frac{\langle \bar{q}q \rangle}{2\pi} \frac{i\gamma_5 \not{q}}{q^2} (s + s') \quad (16)$$

where $\langle \bar{u}u \rangle \simeq \langle \bar{d}d \rangle = \langle \bar{q}q \rangle$ has been used. By means of Cauchy theorem, and assuming global (quark-hadron) duality, one obtains the lowest dimensional FESR

$$g_{\pi NN} = \frac{f_\pi}{8\pi^3} \frac{s_0 s'_0 (s_0 + s'_0)}{\lambda_N^2 M_N} \quad (17)$$

where use has been made of the Gell-Mann, Oakes and Renner relation [16]

$$f_\pi^2 m_\pi^2 = -2m_q \langle \bar{q}q \rangle \quad (18)$$

Since the dispersion in $p^2 = s$ and $p'^2 = s'$ refers to the two nucleonic legs, it is reasonable to assume $s_0 \simeq s'_0$. An analysis of the two-point function involving the nucleonic current $\eta(x)$ [17] in the framework of QCD FESR yields

$$\lambda_N^2 = \frac{s_0^3}{192\pi^4} \quad \lambda_N^2 M_N = -\frac{\langle \bar{q}q \rangle}{8\pi^2} s_0^2 \quad (19)$$

which determines the nucleon mass in terms of s_0 . Conversely, using M_N and $\langle \bar{q}q \rangle$ as input, Eq.(19) fixes λ_N and s_0 . In this fashion, Eq.(17) becomes: $g_{\pi NN} = 48\pi f_\pi / M_N \simeq 15$, not far from the experimental value $g_{\pi NN} \simeq 13$. This level of agreement is more than enough for our purpose here, which is to determine the temperature behaviour of the πNN coupling, i.e. the ratio $g_{\pi NN}(T) / g_{\pi NN}(0)$. To achieve this, we have calculated the thermal corrections to the QCD spectral function with the result

$$Im\Pi(p, p', q) = \frac{1}{4\pi} \langle \bar{q}q \rangle \frac{i\gamma_5 \not{q}}{q^2} \{ p^2 f(p, T) + p'^2 f(p', T) \} \quad (20)$$

where

$$f(p, T) = \int_{-1}^1 dx \left[1 - n_F \left(\frac{|p_0 - |\vec{p}|x|}{2} \right) - n_F \left(\frac{|p_0 + |\vec{p}|x|}{2} \right) \right] \quad (21)$$

and a similar expression for $f(p', T)$. The FESR in this case becomes

$$g_{\pi NN}(T) = \frac{1}{8\pi^3} \frac{f_\pi(T)}{M_N(T) \lambda_N^2(T)} \int_0^{s_0(T)} \int_0^{s'_0(T)} ds ds' [s f(p, T) + s' f(p', T)] \quad (22)$$

where use has been made of the thermal Gell-Mann, Oakes and Renner relation, which has been recently shown to be valid over a wide range of temperatures [18]. The temperature behaviour of f_π , valid up to the critical temperature, has been obtained in [19]. The function $s_0(T)$ has been determined from a FESR for the two-point function involving the axial-vector current [20] - [21]; it scales as: $s_0(T)/s_0(0) \simeq (f_\pi(T)/f_\pi(0))^2$. The thermal nucleonic coupling $\lambda_N(T)$ has been determined from a QCD-FESR in the nucleon channel,

with the result [17]

$$\lambda_N^2(T) = \lambda_N^2(0) \left(\frac{s_0(T)}{s_0(0)} \right)^3 [1 + G_a(T)] \quad (23)$$

where

$$G_a(T) = \frac{576}{(s_0(T))^3} \int_0^{\sqrt{s_0(T)}} d\omega \int_0^{\omega/2} dx \int_{\omega/2-x}^{\omega/2} dy x(\omega - 2x) \{ -n_F(x) - n_F(y) + n_F(x)n_F(y) + n_F(\omega - x - y) [n_F(x) + n_F(y) - 1] \}. \quad (24)$$

and $n_F(z) = (1 + e^{-z/T})^{-1}$ is the Fermi factor. With all this information one can then solve Eq.(22), after choosing a particular Lorentz frame. Our choice is the rest frame of the incoming nucleon, i.e. $\vec{p} = 0$ and $p_0 = \sqrt{s}$, however, the final results are quite insensitive to the choice of frame. The result for the ratio $g_{\pi NN}(T)/g_{\pi NN}(0)$ as a function of T/T_d is shown in Fig.4. One can clearly appreciate the vanishing of this coupling at the critical temperature. This is the temperature at which $f_\pi(T)$ vanishes, i.e. the critical temperature for the chiral-symmetry restoration phase transition, which is basically the same temperature at which $s_0(T)$ vanishes, i.e. the critical temperature for the quark-gluon deconfinement phase transition [20] - [21].

Finally, the mean-square radius associated to the pion-nucleon vertex

$$\langle r_{\pi NN}^2 \rangle_T = 6 \frac{\partial}{\partial q^2} \ln g_{\pi NN}(q^2, T) |_{q^2=0} \quad (25)$$

can be easily calculated, with the result

$$\begin{aligned} \langle r_{\pi NN}^2 \rangle_T &= \left\{ \int_0^{s_0(T)} \int_0^{s'_0(T)} ds ds' \int_{-1}^1 dx \left[s \left(1 - 2n_F(\sqrt{s}/2) \right) + s' \left(1 - 2n_F(z) \right) \right] \right\}^{-1} \\ &\times \frac{6}{2T} \int_0^{s_0(T)} \int_0^{s'_0(T)} ds ds' \frac{1}{\sqrt{s}} \int_{-1}^1 dx n_F^2(z) e^{z/T} \left[1 + x \frac{s + s'}{|s - s'|} \right] \end{aligned} \quad (26)$$

where

$$z = \frac{s + s' + |s - s'|x}{4\sqrt{s}} \quad (27)$$

and the rest frame of the incoming nucleon has been used. A numerical evaluation of Eq.(26) gives the result shown in Fig. 5. Notice that since we have made the pion-pole ap-

proximation, $g_{\pi NN}$ at $T = 0$ is independent of q^2 . The mean-square radius is non-vanishing only at finite temperature, where a q^2 dependence appears through the Fermi factors.

In summary, the vanishing of the pion-nucleon coupling, and the divergence of the associated mean-square radius, at a critical temperature has been shown to follow from the thermal linear sigma model at leading (one-loop) order, as well as from a thermal QCD-FESR. This may be viewed as (analytical) evidence supporting the existence of the quark-gluon deconfinement phase transition. As the critical temperature is approached, the strength of the coupling of pions to nucleons is quenched, and at the same time, the size of the nucleon as probed by the pion gets bigger. The qualitative agreement between the two methods lends further support to the extension of the QCD sum rule program to finite temperature. It should be noticed that potential non-diagonal vacuum condensates [22] do not enter our FESR because of their (higher) dimensionality. We have emphasized many times in the past that QCD-FESR are far better than e.g. QCD-Laplace transform sum rules, to the extent that the lowest dimensional thermal FESR do not involve (unknown) non-diagonal vacuum condensates.

Acknowledgements

This work has been supported in part by the Foundation for Research Development (South Africa), and by Fondecyt (Chile) under grant No. 1950797.

References

- [1] For reviews see e.g. F. Karsch, Nucl. Phys. A 590 (1995) 367; H. Meyer-Ortmanns, Rev. Mod. Phys. 68 (1996) 473.
- [2] H. Leutwyler and A. V. Smilga, Nucl. Phys. B 342 (1990) 302.
- [3] A. Larsen, Z. Phys. C 33 (1986) 291; C. Contreras and M. Loewe, Int. J. Mod. Phys. A 5 (1990) 2297.
- [4] C. A. Dominguez, M. Loewe, and J. C. Rojas, Phys. Lett. B 320 (1994) 377.
- [5] A. I. Bochkarev and M. E. Shaposnikov, Nucl. Phys. B 268 (1986) 220.
- [6] C. A. Dominguez and M. Loewe, Phys. Rev. D 52 (1995) 3143; Z. Phys. C 51 (1991) 69.
- [7] R. D. Pisarski Phys. Lett. B 110 (1982) 155; C. A. Dominguez, Nucl. Phys. B (Proc. Suppl.) 15 (1990) 225; C. A. Dominguez and M. Loewe, Z. Phys. C 49 (1991) 423.
- [8] C. A. Dominguez, M. Loewe, and J. S. Rozowsky, Phys. Lett. B 335 (1994) 506.
- [9] C. A. Dominguez, M. Loewe, and M. S. Fetea, Phys. Lett. B 406 (1997) 149.
- [10] B. W. Lee, *Chiral Dynamics*, Gordon and Breach (New York, 1972).
- [11] J. A. Mignaco and E. Remiddi, Nuovo Cimento 1 A (1971) 376.
- [12] L. Dolan, and R. Jackiw, Phys. Rev. D 9 (1974) 3320.
- [13] C. A. Dominguez, Rivista Nuovo Cimento 8 (1985) 1.
- [14] J. Gasser and H. Leutwyler, Phys. Rep. 87 (1982) 77.
- [15] J. Gasser and H. Leutwyler, Phys. Lett. B 184 (1987) 83.
- [16] M. Gell-Mann, R. Oakes and B. Renner, Phys. Rev. 175 (1968) 2195.
- [17] C. A. Dominguez and M. Loewe, Z. Phys. C 58 (1993) 273.
- [18] C. A. Dominguez, M. Loewe, and M. S. Fetea, Phys. Lett. B 387 (1996) 151.

- [19] A. Barducci, R. Casalbuoni, S. de Curtis, R. Gatto and G. Pettini, Phys. Rev. D 46 (1992) 2203.
- [20] C. A. Dominguez and M. Loewe, Phys. Lett. B 233 (1989) 201.
- [21] A. Barducci, R. Casalbuoni, S. de Curtis, R. Gatto and G. Pettini, Phys. Lett. B 244 (1990) 311.
- [22] T. Hatsuda, Y. Koike and S. H. Lee, Nucl. Phys. B 394 (1993) 221.

Figure Captions

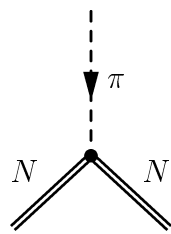
Figure 1. Leading (one-loop) diagrams contributing to $g_{\pi NN}$ in the linear sigma model.

Figure 2. Thermal behaviour of the πNN mean square radius, Eq.(8), in the linear sigma model.

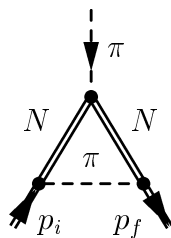
Figure 3. Leading order QCD diagrams entering the determination of the spectral function relevant to $g_{\pi NN}$.

Figure 4. Thermal behaviour of the πNN coupling determined from the QCD-FESR Eq.(22).

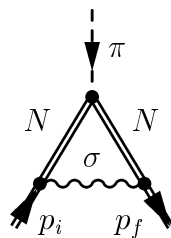
Figure 5. Thermal behaviour of the πNN mean square radius, Eq.(26), according to the QCD-FESR.



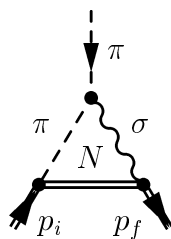
(a)



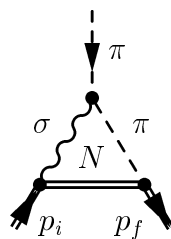
(b)



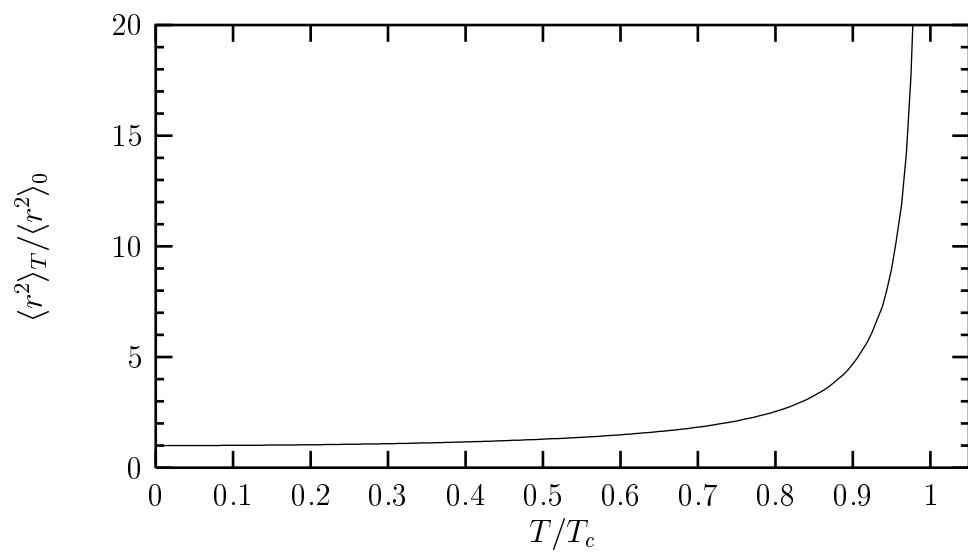
(c)

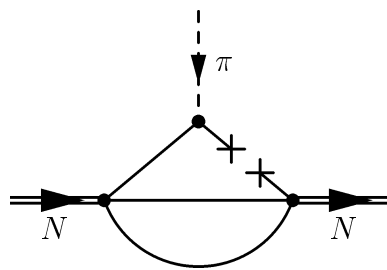


(d)

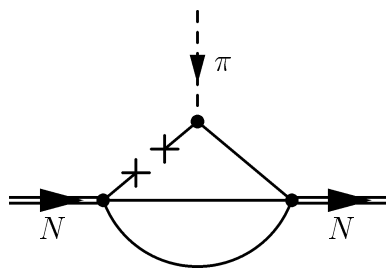


(e)

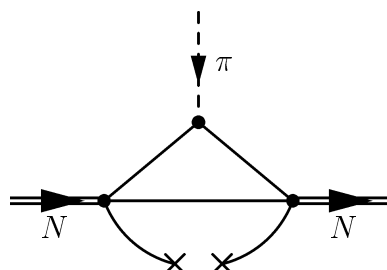




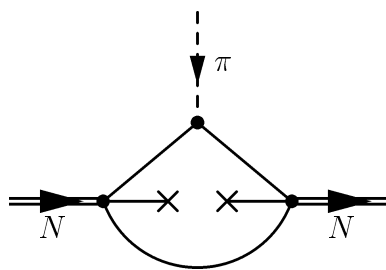
(a)



(b)



(c)



(d)

